JACS
JOURNAL OF THE AMERICAN CHEMICAL SOCIETY

Article

pubs.acs.org/JACS

Enhancing Mechanical Performance of a Covalent Self-Healing Material by Sacrificial Noncovalent Bonds

James A. Neal, Davoud Mozhdehi, and Zhibin Guan*

Department of Chemistry, University of California, Irvine, California 92697, United States

Supporting Information

ABSTRACT: Polymers that repair themselves after mechanical damage can significantly improve their durability and safety. A major goal in the field of self-healing materials is to combine robust mechanical and efficient healing properties. Here, we show that incorporation of sacrificial bonds into a self-repairable network dramatically improves the overall mechanical properties. Specifically, we use simple secondary amide side chains to create dynamic energy dissipative hydrogen bonds in a covalently cross-linked polymer network, which can self-heal via olefin cross-metathesis. We envision that this straightforward sacrificial bonding strategy can be employed to improve mechanical properties in a variety of self-healing systems.

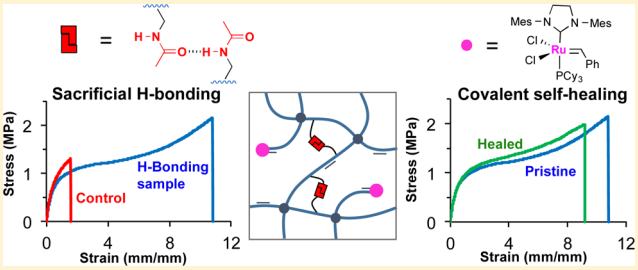

INTRODUCTION

In contrast to biological systems that can spontaneously self-repair, most synthetic materials cannot self-heal following mechanical damage. Mimicking nature's ability to heal would result in new materials with improved durability and safety. A variety of self-healing polymers have been developed. Healing agents[1] as well as reversible covalent[2−12] and noncovalent bonds,[13−19] with stimuli such as heat[4] and light,[15,20] have been used to promote healing. A major challenge in the expanding field of self-healing polymers is to combine robust mechanical properties and high healing efficiency under mild conditions.[21,22] Currently, most spontaneous and intrinsically self-healing materials are limited to relatively weak polymeric systems due to the necessity of high chain dynamics required for healing. The weak mechanical properties of efficient self-healing materials will limit their potential applications.

An important strategy employed in biological materials to enhance mechanical properties is incorporation of sacrificial noncovalent bonds.[23] Noncovalent sacrificial bonds in polymeric materials can efficiently dissipate large amounts of energy through reversible bond rupture, affording a unique combination of high toughness and the ability to reversibly recover after large strain.[24,25] Reversible sacrificial bonds commonly used as transient cross-linkers in synthetic materials include ionic,[26] metal−ligand,[27] and hydrogen-bonding interactions.[28−31] Whereas a few covalent self-healing polymers contain sacrificial bonds,[12] to the best of our knowledge, such sacrificial bond strategy has not been carefully studied nor purposely used to enhance the mechanical properties of self-healing polymers. Herein, we demonstrate that incorporation of a simple, sacrificial hydrogen-bonding amide functionality dramatically enhances the mechanical performance of a covalent self-healing polymeric network (Figure 1).

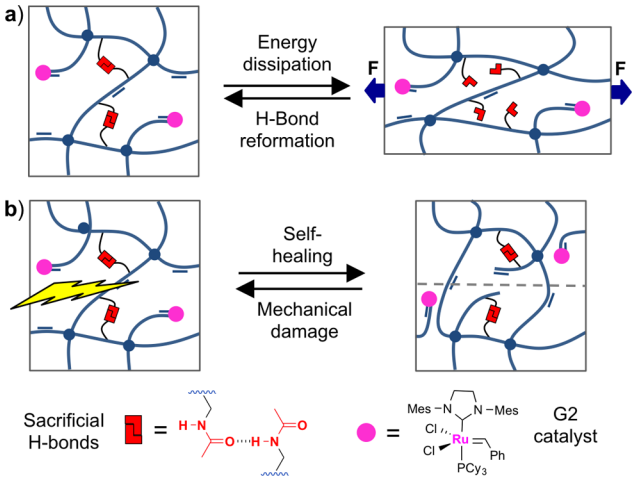

Figure 1. Design concept for (a) reversible, energy dissipative rupture of sacrificial hydrogen bonds in a (b) G2-mediated self-healing olefin-containing network.

The covalent self-healing system we used to illustrate this concept is based on the dynamic olefin metathesis reaction that our laboratory has previously demonstrated for efficient covalent self-healing.[5] Specifically, we introduced secondary amide side chains into a cyclooctene (CO)-based, olefin-containing polymer backbone. After cross-linking the polymer and incorporating the Grubbs' second-generation ruthenium catalyst (G2), a self-healing network was created with both transient and covalent cross-links. Upon stress, the hydrogen bonds are broken to dissipate energy, which results in an increased overall toughness of the material. Due to the

Received: February 12, 2015
Published: March 19, 2015

DOI: 10.1021/jacs.5b01601
J. Am. Chem. Soc. 2015, 137, 4846−4850

reversibility of hydrogen bonds, unloading of stress allows hydrogen bonds to re-form, thereby increasing toughness over multiple loading cycles (Figure 1a). Following mechanical damage, G2-mediated olefin metathesis at the fracture interface results in self-healing (Figure 1b). A secondary amide was used for its dynamic hydrogen-bonding capability,[13] compatibility with G2,[32] and synthetic simplicity.

RESULTS AND DISCUSSION

Synthesis and Characterization. The synthesis of secondary amide-containing CO networks (ACON) is summarized in Scheme 1. First, hydroxylated CO (**2**) was synthesized from cyclooctadiene (COD) via stoichiometrically controlled epoxidation[33] followed by epoxide opening with DIBAL-H (Scheme 1a).[34] From precursor **2**, we prepared the secondary amide-functionalized CO derivative (**3**) via carbodiimide coupling with *N*-acetylglycine.[35] An analogous control monomer was synthesized with the hydrogen-bonding capability blocked through *N*-methylation of the amide group (**4**).

Scheme 1. Synthesis of Cyclooctene Derivatives and Olefin-Containing Polymers[a]

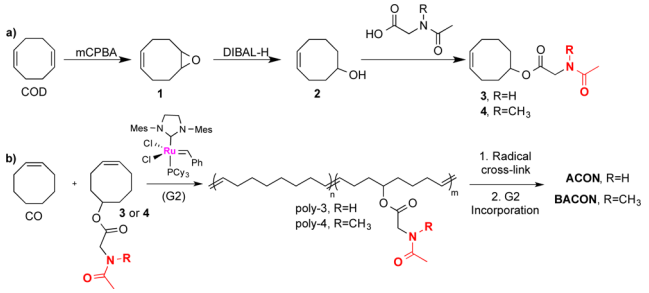

[a](a) Synthesis of hydrogen-bonding cyclooctene derivative **3** and the blocked control derivative **4**. (b) Synthesis of the amide-containing CO network (ACON) and hydrogen-bond-blocked control network (BACON).

ACON was synthesized from monomer **3** via ring-opening metathesis polymerization with G2, a robust and functional-group-tolerant catalyst.[32,36,37] We chose to copolymerize **3** with CO to control the amide mole fraction in ACON (Scheme 1b). Following our reported protocol,[38] the ACON polymer was cross-linked by radical reaction and G2 was incorporated by swelling ([olefin]/[G2] = 2000) to form the ACON network. For comparison, we synthesized a control CO network with the amide hydrogen bond blocked (BACON) through copolymerization of **4** with CO. The properties of both polymer networks are summarized in Table 1. The molecular weights for the hydrogen bonding and control polymers are very close. The small differences in molecular weight should not significantly affect the mechanical properties of the networks because the polymers are covalently cross-linked.[39] ACON was synthesized with incorporation of **3** at 20 mol % because this composition affords a combination of enhanced mechanical properties and efficient healing. Non-cross-linked prepolymers of ACON and BACON possess identical melting transitions (T_m) of ~20 °C. Furthermore, the similar swelling ratios of ACON and BACON indicate that cross-linking densities are nearly identical.

Table 1. Molecular and Physical Characterization of ACON and BACON

sample	mol % of **3** or **4**[a]	M_n[b] (kDa)	M_w/M_n[b]	T_m[c] (°C)	swelling ratio[d]
ACON	20 (**3**)	155	1.69	21.89	4.39 ± 0.07
BACON	20 (**4**)	157	2.10	19.70	4.85 ± 0.08

[a]Estimated from ^{1}H NMR. [b]Determined by size exclusion chromatography using polystyrene standards in THF. [c]Determined via differential scanning calorimetry of polymers before cross-linking. [d]Calculated using ASTM protocol D2765-11.[40]

Mechanical Properties via Uniaxial Tensile Testing. The mechanical properties of ACON and BACON were characterized via static uniaxial tensile testing (Figure 2 and Table 2). We observe a dramatic increase in maximal strain-at-break and toughness after the incorporation of sacrificial hydrogen bonds (Figure 2a). ACON was over 7-fold tougher than the analogous control polymer, illustrating the energy dissipative capability of sacrificial hydrogen bonds. ACON achieved a significantly higher strain-at-break near 950%, while the control network, BACON, extended to only 150%.

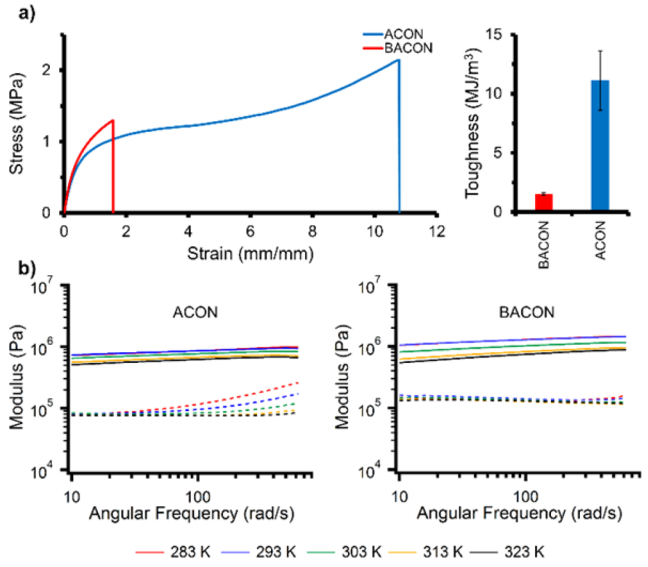

Figure 2. (a) Representative stress–strain curves for ACON and BACON (strain rate: 100 mm/min, 25 °C). Bar graphs summarize the toughness of each sample (three measurements). (b) Isotherm of the storage (solid) and loss (dash) moduli at various frequencies and temperatures for the non-cross-linked ACON (left) and BACON (right) prepolymer samples.

Table 2. Summary of Mechanical and Self-Healing Properties[a]

sample	E[b] (MPa)	tensile strength (MPa)	ε[c] (%)	toughness[d] (MJ/m^3)
ACON	2.34 ± 0.22	1.66 ± 0.35	938 ± 101	11.13 ± 2.51
BACON	2.51 ± 0.10	1.31 ± 0.01	167 ± 9	1.513 ± 0.09
ACON (1 h)[e]	2.15 ± 0.12	1.14 ± 0.15	408 ± 132	3.67 ± 1.57
ACON (3 h)[e]	2.32 ± 0.28	1.65 ± 0.26	835 ± 66	9.75 ± 2.06

[a]All tensile tests were conducted at a strain rate of 100 mm/min, at 25 °C. [b]Young's modulus. [c]Maximum strain-at-break. [d]Calculated by integration of the area under stress–strain curves. [e]Self-healed samples after the designated time.

DOI: 10.1021/jacs.5b01601
J. Am. Chem. Soc. 2015, 137, 4846–4850

Interestingly, the sacrificial bonds do not contribute to the initial stiffness, as the Young's moduli of both networks are near 2.50 MPa. This is in agreement with a previous study on "mechanically invisible" cross-linked gels[27] in which Craig et al. explored transient metal−ligand cross-links that did not contribute to the initial stiffness of the sample but sufficiently dissipated energy to increase the strain-at-break of the material. Presumably, the lifetime for monodendate hydrogen bonds of amides in our system is very short, making them "mechanically invisible" at the time scale of the tensile experiment. Therefore, the transient hydrogen bonds do not contribute to the Young's modulus but increase the strain-at-break and toughness through energy dissipation.

Investigation of Dynamic Sacrificial Bonds via Melt Rheology. To further understand the effect of hydrogen bonds on the dynamic mechanical properties of our system, we surveyed the rheological properties of both non-cross-linked ACON and BACON prepolymers by measuring the storage and loss moduli at various frequencies and temperatures under constant low strain (0.1%). While the storage modulus for both samples remained relatively constant across the frequency range, the loss modulus exhibited a clear frequency-dependent behavior for ACON samples at lower temperatures (Figure 2b, left). Given the high degree of polymerization for both polymers and the relatively low number of hydrogen bonds along the backbone, the storage modulus should be mainly determined by the modulus of the entangled polymer chains.[41,42] However, the sacrificial hydrogen bonds have a more pronounced effect on the frequency dependence of the loss modulus. At low frequencies, hydrogen-bonding kinetics are too fast for efficient energy dissipation. As the frequency is increased to approach the hydrogen-bonding kinetics, dissociation of transient hydrogen bonds and subsequent chain relaxation provides energy dissipation under shear stress, thus contributing to the observed increase in the loss modulus of ACON (Figure 2b, left). A temperature increase perturbs the equilibrium and kinetics of the hydrogen bond association, therefore, reducing their effect on energy dissipation and loss modulus. Consistent with previous reports of functionalized polybutadiene with hydrogen-bonding units,[28,42] the upward transition of loss modulus is shifted to lower frequency by incorporation of hydrogen-bonding units.

Analysis of Sacrificial Bond Recovery via Cyclic Tensile Testing. In practical applications, materials often undergo repeated stress cycles. Therefore, the reversibility and recovery of the sacrificial hydrogen bonds in ACON were probed through cyclic tensile testing (Figure 3). For this study, G2 was not incorporated into the samples to avoid the complication of plastic deformation due to olefin metathesis. ACON was pulled to an extensibility (300%) that would be catastrophic for the control network which breaks at 167% strain. The ACON sample was loaded, unloaded, and *immediately* reloaded 10 times. Significant hysteresis was observed in the first loading−unloading cycle, indicating a large amount of energy dissipation through rupture of multiple hydrogen bonds. However, 80% of the energy dissipation observed in cycle 1 was lost in cycle 2. A similar phenomenon has been observed in other systems containing both hydrogen bond and covalent cross-links[29] and is attributed to the buildup of elastic deformation, which cannot relax to equilibrium on the time scale of individual cycles. Over subsequent cycles (cycles 3−10), the amount of energy dissipation continued to slightly decrease, which we attribute to additional elastic deformation.

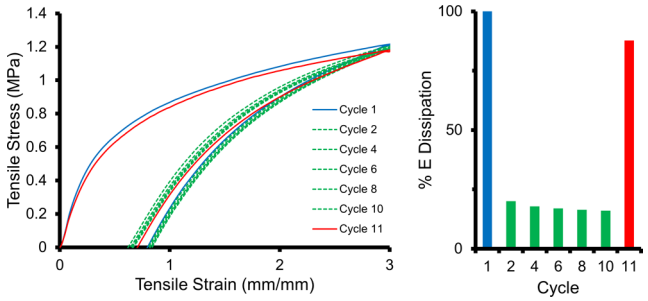

Figure 3. Recovery and cyclic loading of ACON with no G2 incorporation. ACON specimens were loaded (300%), unloaded, and immediately reloaded 10 times (strain rate: 100 mm/min, 25 °C). Cycles 1, 2, 4, 6, 8, 10, and 11 are plotted for clarity. Cycle 11 took place after no stress for 30 min at room temperature. Bar graphs summarize the percent energy dissipation for each sample.

After 10 cycles, ACON was allowed to relax under ambient conditions for 30 min to recover its original length. Cycle 11 shows that ∼90% of the original energy dissipation observed in cycle 1 was recovered in this short time. We propose that the excellent recovery of energy dissipative properties is due to the survival of covalent cross-links, which prevent permanent deformation and assist in the re-formation of sacrificial hydrogen bonds.

Self-Healing Studies. Finally, the self-healing behavior of the ACON sample was investigated by following reported protocols.[43] Previous studies have shown that G2 can tolerate a wide range of polar functional groups including secondary amide groups.[32,36,37] We envisioned that the incorporation of sacrificial hydrogen-bonding secondary amides should not negatively impact olefin cross-metathesis in our bulk samples for self-healing. To test this, ACON samples were damaged (cut through 70−90% of width) and the cut interfaces were brought together with slight pressure for 1 min. The sample was then left to heal at 50 °C in air with no applied pressure for the remainder of the experiment. Moderate heat is required to facilitate ACON healing because the sample is semicrystalline with a broad melting transition in the range of −5 to 40 °C (see Figure S20 in the Supporting Information). The crystallinity reduces chain dynamics and impedes the self-healing process. Heating the sample at 50 °C melts the crystalline phase and enhances the healing ability. After the desired healing time, the extent of healing was quantified via percent recovery of pristine sample toughness (Figure 4a). Each polymer was treated under identical conditions in triplicate to characterize their healing.

Healing experiments confirm that the new system containing sacrificial hydrogen bonds shows excellent healing properties. For all healing times, the stress−strain curves overlap closely with the original samples (Figure 4a). ACON achieved 90% toughness recovery after healing for just 3 h in air at 50 °C. The study suggests that the healing is time-dependent, as 1 h healing achieved near 30% toughness recovery. Additionally, we observe fast and complete recovery of the Young's modulus after just 1 h of healing (Figure 4a, red curve, and Table 2). The healing is through olefin cross-metathesis at the cut interface. For a control study, ACON samples without incorporation of the G2 catalyst show only minimal healing when following an identical protocol (Figure 4b). The efficient healing of ACON samples indicates that G2 turnover frequency is not significantly affected by secondary amide functionality at the tested incorporation ratios of **3**.

DOI: 10.1021/jacs.5b01601
J. Am. Chem. Soc. 2015, 137, 4846−4850

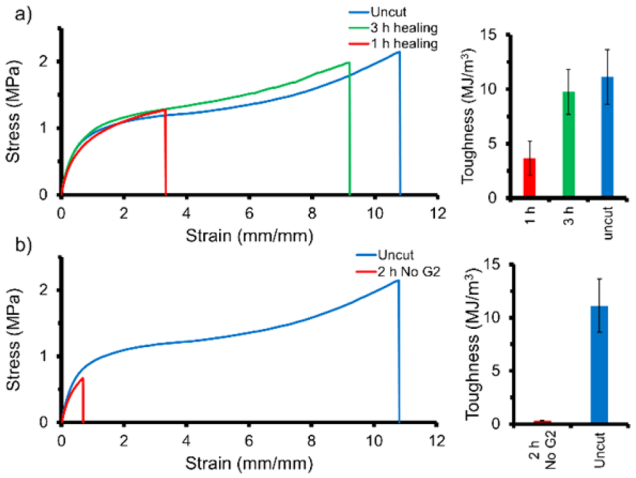

Figure 4. (a) Self-healing experiments for ACON samples at 50 °C in air. (b) Control self-healing experiment for ACON with no G2 incorporation at 50 °C in air. Bar graphs summarize toughness recovery at various time points.

CONCLUSION

In summary, we have demonstrated that sacrificial hydrogen bonds introduced through incorporation of simple secondary amide side chains dramatically improve the mechanical performance of a dynamic covalent self-healing material. By incorporating 20 mol % of our sacrificial hydrogen-bonding monomer (**3**) into an olefin-containing network, the strain-at-break was increased from 150% for the control network to 950%, and the toughness of the network was enhanced by more than 7-fold. Rheological and cyclic tensile experiments were used to further probe the energy dissipation and reversible recovery of the sacrificial hydrogen bonds in our bulk system. Mediated by the G2 catalyst, the olefin-containing network displays efficient healing under relatively mild conditions. The attained robust mechanical properties combined with the efficient self-healing capability are highly desirable for many practical applications. We anticipate that this straightforward sacrificial bonding strategy can be employed to improve mechanical properties of many other self-healing systems. These studies are currently underway, and the results will be disseminated in time.

EXPERIMENTAL METHODS

General. Anhydrous solvents were purified before use through a column of alumina according to the method described by Pangborn et al.[44] Detailed monomer synthesis and characterization can be found in the Supporting Information. A representative polymerization procedure and polymer characterization data can also be found in the Supporting Information.

Representative Cross-Linking Procedure. The cross-linking procedure was adapted from a previously described protocol.[38] After precipitation, the copolymer of CO and **3** (poly-**3**) was redissolved in dichloromethane (DCM) (380 mL). Three aliquots (1.5 mL) of the poly-**3**/DCM solution were collected and dried to calculate total polymer mass (8.04 g). Dicumyl peroxide (0.048 g, 0.178 mmol, [olefin]/[peroxide] = 333) was added to the DCM solution with stirring. The polymer solution was cast in Teflon molds via slow evaporation overnight. The polymer was melt pressed (100 °C) to remove defects and form testable samples. Poly-**3** was cross-linked at 150 °C for 2 h in vacuo. Finally, the mass of each sample was recorded and subsequently swelled in anhydrous DCM overnight to remove unreacted dicumyl peroxide.

Incorporation of G2. The G2 incorporation procedure was adapted from a previously described protocol.[38] After being swelled in anhydrous DCM overnight, the swollen mass of each sample was recorded. The difference in mass between the swollen and dried sample was used to calculate the volume of DCM in each sample. Samples were soaked in a DCM solution of G2 to incorporate the metathesis catalyst ([olefin]/[catalyst] = 2000) into the polymer network. Swollen samples were equilibrated in G2/DCM solution for 1 h in an ethylene glycol/dry ice bath (−16 °C) and subsequently dried in vacuo for 2 h at room temperature.

Uniaxial Tensile Testing. The mechanical properties of polymer samples were measured using an Instron 3365 machine. Standard stress/strain experiments were performed on samples at room temperature. Samples were extended at a rate of 100 mm/min. Each measurement was performed in triplicate to ensure reproducibility. Uncut samples were heated at 50 °C for 3 h to act as pristine controls for healing experiments. The average sample size was 15 mm × 7 mm × 2 mm (length, width, thickness).

Rheological Studies. Rheology data were collected on an AR-G2 rheometer from TA Instruments (20 mm Peltier plate with no solvent trap, stainless steel, 2800 μm gap width). The instrument was equipped with Peltier temperature control system. Frequency sweep experiments were performed at 0.1% strain by varying the frequency between 10 and 628 rad/s at 10−90 °C for each polymer system. Rheological data were reported from 10 to 50 °C. Temperature was increased at increments of 10 °C with 10 min soak time to ensure the complete equilibration of sample temperature.

Cyclic Tensile Testing. The cyclic tensile test was performed using an Instron 3365 machine. Before the experiment, the length of the ACON sample (with no G2 incorporation) was measured. Next, the sample was loaded, unloaded, and immediately reloaded 10 times to 300% extensibility at room temperature. The loading rate remained constant at 100 mm/min. After the initial 10 cycles, the sample was removed from the clamp and allowed to relax at room temperature for 30 min. After the equilibration period, the length of the ACON sample was again measured and found to have relaxed to its original length. An 11th loading cycle was completed to measure the recovery of energy dissipative properties.

Self-Healing Procedure. Samples were cut with a fresh blade (75% of width) through the center and subsequently pushed back together for 1 min. Samples were left to stand in air for the duration of the experiment at 50 °C. Pristine samples were not cut but carried through an otherwise identical procedure. Samples were allowed to equilibrate to room temperature for 10 min before uniaxial tensile testing. Each measurement was performed in triplicate to ensure reproducibility.

ASSOCIATED CONTENT

Supporting Information

Experimental details including synthesis, sample preparation, and characterization. This material is available free of charge via the Internet at http://pubs.acs.org.

AUTHOR INFORMATION

Corresponding Author

*zguan@uci.edu

Notes

The authors declare no competing financial interest.

ACKNOWLEDGMENTS

This work was supported by the U.S. Department of Energy, Division of Materials Sciences, under Award No. DE-FG02-04ER46162. We also thank Materia Inc. for their generous donation of the Grubb's second-generation catalyst.

DOI: 10.1021/jacs.5b01601
J. Am. Chem. Soc. 2015, 137, 4846−4850

REFERENCES

(1) White, S. R.; Sottos, N. R.; Geubelle, P. H.; Moore, J. S.; Kessler, M. R.; Sriram, S. R.; Brown, E. N.; Viswanathan, S. *Nature* **2001**, *409*, 794−797.
(2) Montarnal, D.; Capelot, M.; Tournilhac, F.; Leibler, L. *Science* **2011**, *334*, 965−968.
(3) Capelot, M.; Montarnal, D.; Tournilhac, F.; Leibler, L. *J. Am. Chem. Soc.* **2012**, *134*, 7664−7667.
(4) Chen, X.; Dam, M. A.; Ono, K.; Mal, A.; Shen, H.; Nutt, S. R.; Sheran, K.; Wudl, F. *Science* **2002**, *295*, 1698−1702.
(5) Lu, Y.-X.; Guan, Z. *J. Am. Chem. Soc.* **2012**, *134*, 14226−14231.
(6) Amamoto, Y.; Kamada, J.; Otsuka, H.; Takahara, A.; Matyjaszewski, K. *Angew. Chem., Int. Ed.* **2011**, *50*, 1660−1663.
(7) Imato, K.; Nishihara, M.; Kanehara, T.; Amamoto, Y.; Takahara, A.; Otsuka, H. *Angew. Chem., Int. Ed.* **2012**, *51*, 1138−1142.
(8) Yao, L.; Yuan, Y. C.; Rong, M. Z.; Zhang, M. Q. *Polymer* **2011**, *52*, 3137−3145.
(9) Deng, G.; Tang, C.; Li, F.; Jiang, H.; Chen, Y. *Macromolecules* **2010**, *43*, 1191−1194.
(10) Ying, H.; Zhang, Y.; Cheng, J. *Nat. Commun.* **2014**, *5*, 3218.
(11) Zheng, P.; McCarthy, T. J. *J. Am. Chem. Soc.* **2012**, *134*, 2024−2027.
(12) Martin, R.; Rekondo, A.; Ruiz de Luzuriaga, A.; Cabañero, G.; Grande, H. J.; Odriozola, I. *J. Mater. Chem. A* **2014**, *2*, 5710−5715.
(13) Chen, Y.; Kushner, A. M.; Williams, G. A.; Guan, Z. *Nat. Chem.* **2012**, *4*, 467−472.
(14) Cordier, P.; Tournilhac, F.; Soulié-Ziakovic, C.; Leibler, L. *Nature* **2008**, *451*, 977−980.
(15) Burnworth, M.; Tang, L.; Kumpfer, J. R.; Duncan, A. J.; Beyer, F. L.; Fiore, G. L.; Rowan, S. J.; Weder, C. *Nature* **2011**, *472*, 334−337.
(16) Burattini, S.; Greenland, B. W.; Merino, D. H.; Weng, W.; Seppala, J.; Colquhoun, H. M.; Hayes, W.; MacKay, M. E.; Hamley, I. W.; Rowan, S. J. *J. Am. Chem. Soc.* **2010**, *132*, 12051−12058.
(17) Wang, C.; Liu, N.; Allen, R.; Tok, J. B. H.; Wu, Y.; Zhang, F.; Chen, Y.; Bao, Z. *Adv. Mater.* **2013**, *25*, 5785−5790.
(18) Bode, S.; Zedler, L.; Schacher, F. H.; Dietzek, B.; Schmitt, M.; Popp, J.; Hager, M. D.; Schubert, U. S. *Adv. Mater.* **2013**, *25*, 1634−1638.
(19) Ahn, B. K.; Lee, D. W.; Israelachvili, J. N.; Waite, J. H. *Nat. Mater.* **2014**, *13*, 867−872.
(20) Ghosh, B.; Urban, M. W. *Science* **2009**, *323*, 1458−1460.
(21) Wool, R. P. *Soft Matter* **2008**, *4*, 400−418.
(22) Murphy, E. B.; Wudl, F. *Prog. Polym. Sci.* **2010**, *35*, 223−251.
(23) Fantner, G. E.; Hassenkam, T.; Kindt, J. H.; Weaver, J. C.; Birkedal, H.; Pechenik, L.; Cutroni, J. A.; Cidade, G. A. G.; Stucky, G. D.; Morse, D. E.; Hansma, P. K. *Nat. Mater.* **2005**, *4*, 612−616.
(24) Zhao, X. *Soft Matter* **2014**, *10*, 672−687.
(25) Haque, M. A.; Kurokawa, T.; Gong, J. P. *Polymer* **2012**, *53*, 1805−1822.
(26) Sun, T. L.; Kurokawa, T.; Kuroda, S.; Ihsan, A. B.; Akasaki, T.; Sato, K.; Haque, M. A.; Nakajima, T.; Gong, J. P. *Nat. Mater.* **2013**, *12*, 932−937.
(27) Kean, Z. S.; Hawk, J. L.; Lin, S.; Zhao, X.; Sijbesma, R. P.; Craig, S. L. *Adv. Mater.* **2014**, *26*, 6013−6018.
(28) Müller, M.; Seidel, U.; Stadler, R. *Polymer* **1995**, *36*, 3143−3150.
(29) Zhang, H.; Chen, Y.; Lin, Y.; Fang, X.; Xu, Y.; Ruan, Y.; Weng, W. *Macromolecules* **2014**, *47*, 6783−6790.
(30) Yang, J.; Han, C.-R.; Zhang, X.-M.; Xu, F.; Sun, R.-C. *Macromolecules* **2014**, *47*, 4077−4086.
(31) Kushner, A. M.; Gabuchian, V.; Johnson, E. G.; Guan, Z. *J. Am. Chem. Soc.* **2007**, *129*, 14110−14111.
(32) Shi, H.; Shi, D.; Yin, L.; Luan, S.; Zhao, J.; Yin, J. *React. Funct. Polym.* **2010**, *70*, 449−455.
(33) Allcock, H. R.; Welna, D. T.; Stone, D. A. *Macromolecules* **2005**, *38*, 10406−10412.
(34) Lang, K.; Davis, L.; Wallace, S.; Mahesh, M.; Cox, D. J.; Blackman, M. L.; Fox, J. M.; Chin, J. W. *J. Am. Chem. Soc.* **2012**, *134*, 10317−10320.
(35) Higley, M. N.; Pollino, J. M.; Hollembeak, E.; Weck, M. *Chemistry* **2005**, *11*, 2946−2953.
(36) Scholl, M.; Ding, S.; Lee, C. W.; Grubbs, R. H. *Org. Lett.* **1999**, *1*, 953−956.
(37) Martinez, H.; Ren, N.; Matta, M.; Hillmyer, M. *Polym. Chem.* **2014**, *5*, 3507−3532.
(38) Lu, Y.-X.; Tournilhac, F.; Leibler, L.; Guan, Z. *J. Am. Chem. Soc.* **2012**, *134*, 8424−8427.
(39) Dickie, R. A.; Ferry, J. D. *J. Phys. Chem.* **1966**, *70*, 2594−2600.
(40) ASTM D2765-11, Standard Test Methods for Determination of Gel Content and Swell Ratio of Crosslinked Ethylene Plastics; ASTM International: West Conshohocken, PA, 2006; www.astm.org.
(41) González, A. E. *Polymer* **1983**, *24*, 77−80.
(42) Leibler, L.; Rubinstein, M.; Colby, R. H. *Macromolecules* **1991**, *24*, 4701−4707.
(43) Mozhdehi, D.; Ayala, S.; Cromwell, O. R.; Guan, Z. *J. Am. Chem. Soc.* **2014**, *136*, 16128−16131.
(44) Pangborn, A. B.; Giardello, M. A.; Grubbs, R. H.; Rosen, R. K.; Timmers, F. J. *Organometallics* **1996**, *15*, 1518−1520.

DOI: 10.1021/jacs.5b01601
J. Am. Chem. Soc. 2015, 137, 4846−4850